A minute magneto hydro dynamic (MHD) mixer — **Source link** ⧉

Haim H. Bau, Jihua Zhong, Mingqiang Yi

Institutions: University of Pennsylvania

Related papers:

- Chaotic Mixer for Microchannels

- Electrokinetic instability micromixer

- Micromixers?a review

- Passive mixing in a three-dimensional serpentine microchannel

- Ultrasonic micromixer for microfluidic systems

Share this paper: 🄵 🆃 🇮🇳 ✉

View more about this paper here: https://typeset.io/papers/a-minute-magneto-hydro-dynamic-mhd-mixer-25amgl8tgk

Departmental Papers (MEAM)

Department of Mechanical Engineering &
Applied Mechanics

October 2001

A minute magneto hydro dynamic (MHD) mixer

Haim H. Bau
University of Pennsylvania, bau@seas.upenn.edu

Jihua Zhong
University of Pennsylvania

Mingqiang Yi
University of Pennsylvania

Follow this and additional works at: https://repository.upenn.edu/meam_papers

A minute magneto hydro dynamic (MHD) mixer

Abstract

A theoretical and experimental investigation of a magneto hydrodynamic stirrer is presented. Such a stirrer can be used to enhance mixing in micro total analysis systems. The stirrer utilizes arrays of electrodes deposited on a conduit's walls. The conduit is filled with an electrolyte solution. By applying alternating potential differences across pairs of electrodes, currents are induced in various directions in the solution. In the presence of a magnetic field, the coupling between the magnetic and electric fields induces body (Lorentz) forces in the fluid. Since the electrodes can be patterned in various ways, fairly complex flow fields can be generated. In particular, in this paper, we describe the induction of cellular motion. This motion can be used to deform and stretch material interfaces and to enhance mixing. The MHD stirrer does not utilize any moving parts. The experimental observations are in good agreement with theoretical predictions.

Keywords

Comments

A Minute Magneto Hydro Dynamic (MHD) Mixer

Haim H. Bau[*], Jihua Zhong, and Mingqiang Yi
Dept. Mechanical Engineering and Applied Mechanics
University of Pennsylvania
Philadelphia, PA 19104-6315

ABSTRACT

A theoretical and experimental investigation of a magneto hydrodynamic stirrer is presented. Such a stirrer can be used to enhance mixing in micro total analysis systems. The stirrer utilizes arrays of electrodes deposited on a conduit's walls. The conduit is filled with an electrolyte solution. By applying alternating potential differences across pairs of electrodes, currents are induced in various directions in the solution. In the presence of a magnetic field, the coupling between the magnetic and electric fields induces body (Lorentz) forces in the fluid. Since the electrodes can be patterned in various ways, fairly complex flow fields can be generated. In particular, in this paper, we describe the induction of cellular motion. This motion can be used to deform and stretch material interfaces and to enhance mixing. The MHD stirrer does not utilize any moving parts. The experimental observations are in good agreement with theoretical predictions.

Keywords: Minute Stirrer, Micro mixer, Magneto Hydro Dynamics, MHD

---

[*] All correspondence should be directed to this author. E-mail address: bau@seas.upenn.edu

1. INTRODUCTION

In recent years, there has been a growing interest in developing minute laboratories on a "chip". Often, in order to facilitate chemical and biological reactions, one needs to mix various reagents and chemicals. Although the characteristic lengths associated with micro-devices are small, typically on the order of 100μm, in the case of large molecules, diffusion alone does not provide a sufficiently rapid means for mixing. For example, at room temperature, myosin's coefficient of diffusion in water is about $10^{-11}m^2/s$, and the time constant for diffusion along a length of 100μm is an intolerably large 10^3s. Commonly, one encounters only low Reynolds number flows in micro devices, and turbulence is not available to enhance mixing. Moreover, often it is not feasible to incorporate moving components such as stirrers into microdevices. Thus, one is forced to look for alternatives in order to make the mixing process more efficient.

In view of the above, it is not surprising that many investigators have studied a variety of schemes to enhance mixing. For example, Stremler et. al. (2000), Liu et. al. (2000), and Yi and Bau (2000) micro-fabricated two and three-dimensional "twisted" conduits in polydimethylsiloxane (PMDS), silicon, and low temperature co-fired ceramic tapes, respectively. These "mixers" consisted of sequences of short, straight conduits having rectangular cross-sections. Each conduit formed a 90-degree angle with the preceding one. The bends induced two counter-rotating vortices that deformed material lines and enhanced stirring. For these devices to work effectively, the Reynolds number must be on the order of 10. Unfortunately, many microfluidic systems operate at much lower Reynolds numbers than 10. Moroney et. al. (1991), Selverov and Stone (2000) and Yi, Bau, and Hu (2000) studied stirrers in which travelling waves were induced in a cavity's wall(s). These travelling waves induced peristaltic motion in the confined liquid that facilitated fluid circulation. Another idea was put forward by Lee, et. al., (2000) and others who used two solenoid valves to generate pressure perturbations in the base flow at a desired frequency and amplitude. Effective mixing has been observed, albeit at relatively high Reynolds numbers (On the order of 10) and at fairly significant pressure perturbations.

In this paper, we describe a novel, simple magneto hydrodynamic mixer. Despite their unfavorable scaling (the magnitude of the magnetic forces are proportional to the fluid volume), magnetic forces offer many advantages for microdevices. In many cases, one operates with liquids that are at least slightly conductive such as biological fluids. By patterning electrodes in the flow conduits and subjecting these electrodes to potential differences, one can induce electric currents in the liquid. In the presence of a magnetic force, the currents lead to the generation of a

Bau, H., H., Zhong, J., and Yi, M., 2001, A Minute Magneto Hydro Dynamic (MHD) Mixer, <u>Sensors and Actuators</u> B, 79/2-3, 205-213.

Lorentz force in a direction that is perpendicular to both the magnetic and electric fields. The magnetic field can be induced either internally by coils and soft magnetic material or a magnet embedded inside the device or externally with the use of electromagnets or permanent magnets.

The idea of using magneto hydrodynamic forces for pumping and propulsion is not new. In previous works pertaining to microfluidic systems, Jang and Lee (2000), Lemoff and Lee (2000), and Zhong, Yi, and Bau (2001), among others, positioned electrodes parallel to the conduit walls. The conduits were filled with electrolyte solution. When the electrodes were subjected to a potential difference in the presence of a magnetic field, the resulting Lorentz forces induced fluid motion along the conduit's axis.

In this paper, we use a slightly different idea. Instead of positioning electrodes parallel to the conduit walls, we deposit arrays of electrodes on the conduit's surface in the transverse direction. By subjecting these electrodes to varying potential differences in the presence of a magnetic field, we generate forces that drive fluid flow in various directions in "virtual" wall-less conduits whose geometry is dictated by the positioning of the electrodes. We utilize these idea to generate secondary flows such as may enhance mixing.

In the first part of the paper, we describe the theory of operation of such a stirrer. In the second part of the paper, we describe a simple prototype of such a mixer. Although the mixer can be fabricated with different substrate materials ranging from silicon to ceramic tapes, we found it particularly advantageous to fabricate our prototype with low temperature ceramic tapes (LTCC). LTCCs offer a rapid and inexpensive means of fabricating small and moderate quantities of devices.

2. **THEORY**

The stirrer consists of a liquid-filled conduit having a rectangular cross-section. Figs. 1 and 2 depict, respectively, a schematic top view and a cross-section of the conduit. The x-coordinate is parallel to the conduit's walls. Uniformly spaced electrodes (denoted by the letters A, B, C, D, and E in Fig. 1) are deposited perpendicular to the conduit's walls. It is also possible to deposit electrodes on the conduit's top or in different patterns than depicted in Fig. 1. The electrodes are connected alternately to the positive and negative poles of a DC power supply. As a result, electric current of density $\vec{\mathbf{J}}$ flows in the liquid. The direction of the electric current varies from one location to another as indicated by the hollow arrows in the figure. The liquid is subjected to a uniform magnetic field of intensity ($\vec{\mathbf{B}}$) normal to the conduit's bottom and directed out of the page. The coupling between the

Bau, H., H., Zhong, J., and Yi, M., 2001, A Minute Magneto Hydro Dynamic (MHD) Mixer, <u>Sensors and Actuators</u> B, 79/2-3, 205-213.

magnetic and electric fields induces a body (Lorentz) force, $\vec{J} \times \vec{B}$, that is perpendicular to both $\vec{J}$ and $\vec{B}$ and is directed towards the conduit's side wall. The direction of the force alternates. For example, in the conduit segment between electrodes C and D, the force is directed in the positive y-direction while in the conduit segment between the electrodes B and C, the force is directed in the opposite direction. Consequently, in the conduit segments BC and CD, the liquid will, respectively, move upwards and downwards. The net effect will be the formation of convective cells or eddies. We will show later that these eddies can deform and stretch material lines and stir the fluid.

We denote the conduit's height as 2h, its width as W and the distance between adjacent electrodes as L (see Figs. 1 and 2). When the conduit is relatively long and equipped with a large number of electrodes, we may assume that the phenomenon is periodic in the x-direction. Accordingly, we will analyze a single "cell" containing a single electrode, i.e., the region enclosed between the two symmetry lines and containing electrode C in Fig. 1. The width of this cell is L.

The fluid motion is governed by the Navier-Stokes equation (Batchlor, 1967) with a magnetic body force,

$$\rho \frac{\partial \vec{u}}{\partial t} + \rho(\vec{u} \bullet \nabla)\vec{u} = -\nabla P + \mu \nabla^2 \vec{u} + \vec{J} \times \vec{B}, \tag{1}$$

and the continuity equation:

$$\nabla \bullet \vec{u} = 0. \tag{2}$$

In the above, ρ is the liquid density, $\vec{u}$ is the velocity vector, t is time, P is the thermodynamic pressure, and μ is the shear viscosity. We are neglecting gravitational effects. Ohm's law states that

$$\vec{J} = \sigma(\vec{E} + \vec{u} \times \vec{B}), \tag{3}$$

where σ is the liquid's conductivity.

Although this is not always the case in micro devices, for simplicity's sake and to allow us to illustrate the phenomenon of interest more clearly, we will assume that L and W are of the same order of magnitude and that h<<L. This latter assumption allows us to use "lubrication theory" or "Hele-Shaw" approximation (Batchlor, 1967, p. 222). When $\frac{h}{L} << 1$ and to the first order of approximation (i.e., neglecting terms of order h/L) the pressure

Bau, H., H., Zhong, J., and Yi, M., 2001, A Minute Magneto Hydro Dynamic (MHD) Mixer, Sensors and Actuators B, 79/2-3, 205-213.

$P \sim P(x, y)$ is independent of the z-coordinate and the z-component of the velocity, $u_z=0$. Consequently, the horizontal components of the velocity in the x and y directions can be expressed as

$$\vec{\mathbf{u}} = \left(u^*(x, y)\hat{e}_x + v^*(x, y)\hat{e}_y\right)f(z), \tag{4}$$

where $f(z) = 1 - \left(\dfrac{z}{h}\right)^2$. $\hat{e}_x$ and $\hat{e}_y$ are, respectively, unit vectors in the x and y directions. We substitute $\vec{\mathbf{u}}$ into equation (1) and integrate the equation over the z coordinate. The resulting dimensionless momentum equations are:

$$St^2\frac{\partial u}{\partial t} + \mathrm{Re}\left(\frac{h}{L}\right)\left(\frac{8}{15}\right)\left(u\frac{\partial u}{\partial x} + v\frac{\partial u}{\partial y}\right) = -\frac{\partial p}{\partial x} + \left(\frac{2}{3}\right)\left(\frac{\partial^2 u}{\partial x^2} + \frac{\partial^2 u}{\partial y^2}\right) - 2u, \tag{5}$$

and

$$St^2\frac{\partial v}{\partial t} + \mathrm{Re}\left(\frac{h}{L}\right)\left(\frac{8}{15}\right)\left(u\frac{\partial v}{\partial x} + v\frac{\partial v}{\partial y}\right) = -\frac{\partial p}{\partial y} + \left(\frac{2}{3}\right)\left(\frac{\partial^2 v}{\partial x^2} + \frac{\partial^2 v}{\partial y^2}\right) - 2v + \left(1 + Ha^2 v\right)Sign(x). \tag{6}$$

In the above, the LHS and RHS of the equations represent, respectively, the rate of change in momentum and the various forces (pressure, viscous, and magnetic) acting on the fluid. The Sign(x) function is attached to the magnetic force term to reflect the fact that this force is directed in opposite directions when x<0 and x>0. The equations are valid over the domain $-\dfrac{L}{2} \le x \le \dfrac{L}{2}$ and $-\dfrac{W}{2} \le x \le \dfrac{W}{2}$. The boundary conditions are:

$$u(x,\pm\frac{W}{2}) = v(x,\pm\frac{W}{2}) = u(\pm\frac{L}{2}, y) = \frac{\partial}{\partial x}v(\pm\frac{L}{2}, y) = 0. \tag{7}$$

In the above, we use, respectively, h, $U=\sigma EBh^2/\mu$ and $\mu U/h$ as the length, velocity, and pressure scales. $\mathrm{Re}=UL/\nu$ is the Reynolds number; $St = h\sqrt{\dfrac{4}{3}\dfrac{\omega}{\nu}}$ is the Stanton number; $Ha = hB\sqrt{\dfrac{\sigma}{\mu}}$ is the Hartman number; ω is the frequency of time-wise variations in the electric field; and

$$Sign(x) = \begin{cases} -1 & when\ x > 0 \\ 0 & when\ x = 0 \, . \\ 1 & when\ x < 0 \end{cases} \tag{8}$$

Bau, H., H., Zhong, J., and Yi, M., 2001, A Minute Magneto Hydro Dynamic (MHD) Mixer, Sensors and Actuators B, 79/2-3, 205-213.

Since the width of the electrode is typically small compared to the other characteristic dimensions, we assume in the analysis that the electrodes have zero width. This assumption can be relaxed at the expense of more cumbersome analysis. In what follows, we find it convenient to expand Sign(x) into the Fourier series,

$$Sign(x) \sim \frac{4}{\pi} \sum_{n=0}^{\infty} \left(\frac{1}{1+2n} \right) \sin \left((2n+1)\pi \frac{x}{L} \right). \tag{9}$$

Typically, for non-metallic liquids, Ha<<1. For example, for saline solutions Ha~10^{-3}. Moreover, consistent with our assumption of h/L<<1, we can ignore the nonlinear terms in equations (5) and (6). Finally, we will consider the time-independent case and set St=0. In terms of the stream function Ψ, ($u = \frac{\partial \Psi}{\partial y}$ and $v = -\frac{\partial \Psi}{\partial x}$), the steady state version of equations (5) and (6) can be rewritten compactly as:

$$\nabla^4 \Psi - 3\nabla^2 \Psi = \frac{6}{L} \sum_{n=0}^{\infty} \cos \left((2n+1)\pi \frac{x}{L} \right) \tag{10}$$

with the boundary conditions,

$$\Psi(x, \pm \frac{W}{2}) = \Psi(\pm \frac{L}{2}, y) = \frac{\partial}{\partial y} \Psi(x, \pm \frac{W}{2}) = \frac{\partial^2}{\partial x^2} \Psi(\pm \frac{L}{2}, y) = 0. \tag{11}$$

Equations (10) and (11) are conveniently solved with Mathematica (Wolfram, 1996).

$$\Psi = \sum_{n=0}^{\infty} \left(A_n \left(\cosh(m_1 y) - R_n \cosh(m_2 y) \right) + \frac{6L^3}{\pi^2 (1+2n)^2 (3L^2 + \pi^2 (1+2n)^2)} \right) \cos \left(\frac{(1+2n)\pi}{L} x \right), \tag{12}$$

where

$$A_n = \frac{6L^3 m_2 \sinh(m_2 \frac{W}{2})}{\pi^2 (1+2n)^2 (3L^2 + \pi^2 (1+2n)^2)} \left(m_1 \cosh(m_2 \frac{W}{2}) \sinh(m_1 \frac{W}{2}) - m_2 \cosh(m_1 \frac{W}{2}) \sinh(m_2 \frac{W}{2}) \right)$$

$$R_n = \frac{m_1}{m_2} \frac{\sinh \left(m_1 \frac{W}{2} \right)}{\sinh \left(m_2 \frac{W}{2} \right)}, \quad m_1 = \frac{\pi(1+2n)}{L}, \quad \text{and} \quad m_2 = \sqrt{3 + \left(\frac{m_1}{L} \right)^2}.$$

The series converges reasonably fast at the rate of n^{-4}. When L=W=10, Fig. 3 depicts the variations in the stream function value, $\left| (\Psi(0,0) - \Psi_e(0,0)) / \Psi_e(0,0) \right|$, as a function of the number of terms in the series on a semi-log

scale. In the above, Ψ_e=1.270 denotes the stream function value when 100 terms are used in the summation. The figure indicates that 9 terms in the series are sufficient to obtain a precision better than 0.1%. It is an easy matter to obtain the two velocity components, u and v, and the pressure field from the stream function. In the interest of conciseness, explicit expressions are not given here. The Mathematica notebook is available from the lead author upon request.

When L=W=10, Figs. 4, 5, 6, 7 and 8 depict contours of constant stream lines which also represent particle trajectories, the horizontal velocity u(0,y) as a function of y, the vertical velocity v(x,0) as a function of x, constant pressure contour lines, and the pressure distribution p(x, y) as a function of x and y. As is evident from Figs. 4-6, the magnetic forces induce circulatory motion in the cell. Somewhat surprisingly, the vertical velocity v(x,0) initially increases as x increases, attains a maximum at x~1.39, and then decreases again. This decrease in the v-component of the velocity is a result of the increase of pressure at the stagnation point, $(x, y) = (\dfrac{L}{2}, \dfrac{W}{2})$, as is evident in Figs. 7 and 8. Since the absolute pressure cannot be uniquely determined and it is of no consequence in the case of incompressible flow, we normalized the pressure so that p(0,0)=0.

In order to evaluate the performance of the device as a stirrer, we compute the stretching rate of material interfaces. Consider a stirrer that is filled with two immiscible fluids; one fluid initially occupies the region y<0 and the other fluid occupies the region y>0. y=0 forms an interfacial line between the two fluids. We track the deformation of this interface. To this end, we track particles that are initially located on y=0. Using a 4th order Runge-Kutta procedure, we integrate the advection equations,

$$\frac{dx}{dt} = u(x, y) \quad \text{and} \quad \frac{dy}{dt} = v(x, y), \tag{13}$$

with the initial conditions $-L/2 \le x(0) \le L/2$, $x(0)=x_0$ and y(0)=0. Here, we use $\mu/(\sigma EBh)$ as the time scale. Although all these particles follow the streamlines, they do so at different rates. As a result, the interface is being stretched and deformed. The locations of the interface at various times t=0, 10, 20, 30, 40, and 50 are depicted in Fig. 10. As time goes by, the interface elongates and deforms.

Bau, H., H., Zhong, J., and Yi, M., 2001, A Minute Magneto Hydro Dynamic (MHD) Mixer, <u>Sensors and Actuators</u> B, 79/2-3, 205-213.

Fig. 11 quantifies the stretching of the interface. The figure depicts the normalized length ($IL = \frac{\ell(t)}{L}$) as

a function of time. In the above, $\ell(t)$ is the length of the interface at time t. The symbols and the solid line

correspond, respectively, to computational data and a line of best fit. The data correlates well with the formula:

$$IL \sim 1 + 0.03 \ (t+1) \ ln(t+1). \tag{14}$$

In other words, the length of the interface increases slightly faster than a linear function of time. This is much better

than the rate of increase due to diffusion alone ($t^{1/2}$) but falls short of the exponential rate exhibited by chaotic

advection.

3. EXPERIMENTS

To illustrate that the ideas articulated here can, indeed, be put into practice, we fabricated a crude MHD

stirrer. Although the stirrer can be fabricated with various substrate materials ranging from silicon to polymers, we

chose to construct our prototype with low temperature co-fired ceramic tapes (LTCC). The tapes facilitate easy,

inexpensive, layered manufacturing. They provide a rapid platform for the integration of passive electronics and

fluidics.

In their pre-fired (green) state, the ceramic tapes consist of oxide particles, glass frit, and organic binder

(that can be made from photo-resist). The tapes are typically cast with a thickness starting at 40μm. The pre-fired

tapes can be machined by laser, milling, and photolithography (when the binder is photo-resist). Metallic paths can

be either printed or processed photolithographically to form electrodes, resistors, conductors, and thermistors.

Conduit sizes may range from ~10μm to a few millimeters. Upon firing, the organic binder burns out, the oxide-

particles sinter, and the tapes solidify. Many tapes (>80) can be stacked together, aligned, laminated, and co-fired to

form monolithic structures with complex, three-dimensional mazes of fluidic conduits, electronic circuits, and

electrodes. Glass windows and other materials can be readily attached to the tapes to facilitate optical paths.

Multiple layers of coils can be embedded in the tapes to generate magnetic fields. For additional details, see Bau et.

al. (1998) and Kim et. al. (1998).

The prototype of the stirrer was fabricated with DuPont, LTCC 951AT tapes that have a nominal thickness

of ~250μm. Rectangles of desired size were blanked from the raw material (see Fig. 12). 20μm thick and 700μm

wide DuPont 5734 gold paste was hand-printed at distances 3.3mm apart to form the electrode pattern on layer (1).

Bau, H., H., Zhong, J., and Yi, M., 2001, A Minute Magneto Hydro Dynamic (MHD) Mixer, <u>Sensors and Actuators</u> B, 79/2-3, 205-213.

Although it is possible to control each electrode independently, here we connected three electrodes to a single conductor and two other electrodes to a second conductor. Five additional layers of type 2 (the layer denoted as 2 in Fig. 12) were first laminated and then machined with a numerically controlled milling machine to accommodate an inner cavity and vias (the circular holes) for electric leads. The vias were filled with DuPont 6141 paste and terminated with soldering pads (DuPont 6146). The cavity can be encapsulated with another layer of tape (i.e., layer 3). In the actual experiments, to facilitate flow visualization, we left the cavity uncapped. Subsequent to the machining, the various layers were aligned, stacked, laminated, and co-fired to form a monolithic block. The post-fired cavity (that was formed from 5 layers of type 2) was 1mm deep, 4.7mm wide, and 22.3 mm long.

The cross-section of the assembled device is shown in Fig. 13. In our experiments, we positioned a rectangular, permanent Neodymium magnet (Edmund Scientific, serial number CR81-237, load-carrying capacity of 12-15lb) under the device. The dimensions of the magnet were significantly larger than the cavity's dimensions so that an approximately uniform magnetic field resulted. The magnetic field can also be generated by other means such as an external electromagnet or coils embedded in the ceramic tapes. In the latter case, soft magnetic material such as permalloy can be encapsulated in the tapes to intensify the field.

In the experiments, we filled the cavity with deionized water. The resistance between the electrodes was measured in situ and the conductance was estimated to be $\sigma=2.23\times10^{-4}$ $(\Omega\bullet m)^{-1}$. This conductance accounts for possible dissolution of electrode materials in the water. The leads were connected to a power supply (HP 6032A) that was operated at constant voltage mode. Due to the extremely low currents, it was not possible to operate this power supply at a constant current mode. The very low specific conductivity liquid allowed us to keep the fluid velocity very low and carry out observations using relatively primitive means. With a syringe, we applied a thin trace of dye (Water Soluble Fluorescent Liquid Dye, Model 298-16-Red, Cole Palmer Instrument Company, Niles, Illinois, USA) across the cavity (Fig. 14) and then applied 4V across the electrodes. The current was on the order of μA, and well below the resolution level of our power supply (10mA).

As a result of the application of a DC potential difference across the electrodes, clearly visible fluid flow was induced in the cavity. The motion consisted of rotating cells with the fluid moving up in one interval between two electrodes and down in the adjacent interval. Figs. 15a, b, c, and d depict the deformation of the dye induced by this fluid motion. Depending on the polarity of the electrodes, the dye either moved upwards or downwards (Fig. 15a). This well organized motion could not possibly have been caused by diffusion, and it clearly demonstrates the

Bau, H., H., Zhong, J., and Yi, M., 2001, A Minute Magneto Hydro Dynamic (MHD) Mixer, Sensors and Actuators B, 79/2-3, 205-213.

presence of upward and downward flows in different sections of the cavity. After a few seconds, the polarity of the electrodes was reversed. Since diffusion is relatively slow and the flow is at a relatively low Reynolds number (creeping flow), the dye "retracted its steps" in almost a reversible fashion (Fig. 15b) and then started deforming in the opposite direction (Fig. 15c). When the process was allowed to continue for some time, the dye traced the convective cells in good qualitative agreement with the theoretical predictions of the previous section.

In order to carry out an order of magnitude comparison with theoretical predictions, we computed the approximate time (T) that it takes a segment of dye located midway between the electrodes to move from location $y = -0.4W$ to location $y = 0.4W$. In order to carry out this calculation, we took into consideration the fact that the vertical component of the velocity varies spatially, i.e.,

$$T = \int_{-0.4W}^{0.4W} \frac{dy}{v(\frac{L}{2}, y)}.$$

Numerical integration leads to $T \sim 29$ dimensionless time units. The experimentally measured time corresponded to about 40 time units. This relatively large discrepancy may have been caused because we overestimated the strength of the magnetic field. Moreover, there are a number of differences between the mathematical model and the experiment. For example, the model assumes that the current in the liquid is uniform while in reality there was a more complicated current distribution given the fact that the electrodes were located on the conduit's bottom. If we were to use saline solution instead of de-ionized water, the process would have occurred at least ten times faster.

At the very low currents that we used in our experiments, we did not observe any bubble generation. Bubble generation and electrode deterioration are likely to be a problem when higher voltages or higher conductivity solutions are used. To prevent these undesirable effects, one can employ AC currents. By appropriate synchronization of the electromagnetic field with the AC current, the direction of the Lorentz force would remain unaltered (Lemoff and Lee, 2000).

4. CONCLUSIONS

We have demonstrated in theory and experiment that magneto-electric forces can be used to generate complex motions in electrolytic solutions. We have applied time-independent forces to induce cellular convection in a conduit. The cellular motion stretches and deforms material lines. This process enhances mixing. The rate of deformation as a function of time is slightly faster than linear.

Bau, H., H., Zhong, J., and Yi, M., 2001, A Minute Magneto Hydro Dynamic (MHD) Mixer, <u>Sensors and Actuators</u> B, 79/2-3, 205-213.

Photolithography and screen-printing allow us to form complicated electrode patterns. The interplay between the magnetic and the electric fields provides one with the means of controlling locally the direction and magnitude of the volumetric forces and, in turn, inducing desired flow patterns. In other words, MHD provides the designer of microfluidic systems with a great amount of design flexibility. In this paper, we have described just one simple example of inducing cellular convection in a conduit. The next challenge is to devise time-dependent variations in the magnetic forces and/or electric field that will allow us to obtain a faster, perhaps exponential, rate of stretching of material lines as is common in the case of chaotic advection.

ACKNOWLEDGMENTS

REFERENCES

Batchlor, G., K., 1967, <u>An Introduction to Fluid Dynamics</u>, Cambridge Univ. Press.

Bau, H., Ananthasuresh, G., K., Santiago-Aviles, J., J., Zhong, J., Kim, M., Yi, M., Espinoza-Vallejos, P., 1998, "Ceramic Tape-Based Systems Technology." <u>Micro-Electro-Mechanical Systems (MEMS)</u>, DSC-Vol. 66, 491-498.

Jang J., Lee, S., S., 2000, Theoretical and Experimental Study of MHD (Magnetohydrodynamic) Micropump, <u>Sensors and Actuators A</u>, 80, 84-89.

Kim, M., Yi, M., Zhong, J., Bau, H., Hu, H., Ananthasuresh, G.K., 1998, "The Fabrication of Flow Conduits in Ceramic Tapes and the Measurement of Fluid Flow Through These Conduits." <u>Micro-Electro-Mechanical Systems (MEMS)</u>, DSC-Vol. 66, 171-177.

Lee, Y-K., Tabeling, P., Shih, C., Ho, C-M, 2000, Characterization of MEMS-Fabricated Mixing Device, <u>ASME, IMECE 2000, MEMS 2</u>, 505-511, Orlando, Florida.

Lemoff, A., V., Lee, A., P., 2000, An AC Magentohydrodynamic Micropump, <u>Sensors and Actuators B</u>, 63, 178-185.

Liu, R. H., M. A. Stremler, K. V. Sharp, M. G. Olsen, J. G. Santiago, R. J. Adrian, H. Aref and D. J. Beebe, Passive Mixing in a Three-Dimensional Serpentine Microchannel, <u>Journal of Microelectromechanical Systems</u>, in press, 2000.

Moroney, R. M., White, R., M., Howe, R., T., 1991, Ultrasonically Induced Microtransport, <u>Proceedings IEEE Workshop Micro Electro Mechanical Systems</u>, MEMS 95 Amsterdam, 277-282.

Selverov, K., and Stone, H., A., 2000, Peristaltically Driven Flows for Micro Mixers, to be published in <u>Physics of Fluids</u>.

Bau, H., H., Zhong, J., and Yi, M., 2001, A Minute Magneto Hydro Dynamic (MHD) Mixer, Sensors and Actuators B, 79/2-3, 205-213.

Stremler, M. A., M. G. Olsen, R. J. Adrian, H. Aref, and D. J. Beebe, Chaotic Mixing in Microfluidic Systems, Solid-State Sensor and Actuator Workshop, Hilton Head, SC, June 4-8, 2000.

Wolfram, S., 1996, Mathematica, Cambridge.

Yi, M. and Bau, H.H., 2000, The Kinematics of Bend-Induced Mixing in Micro-Conduits, ASME, IMECE 2000, MEMS 2, 489-496, Orlando, Florida.

Yi, M., Bau, H.H., and Hu, H., 2000, A Peristaltic Meso-Scale Mixer, ASME, IMECE 2000, MEMS 2, 367-374, Orlando, Florida.

Zhong, J., Yi, M., and Bau, H., H., 2001, A Magnetohydrodynamic Pump Fabricated with Ceramic Tapes, submitted for publication.

Bau, H., H., Zhong, J., and Yi, M., 2001, A Minute Magneto Hydro Dynamic (MHD) Mixer, <u>Sensors and Actuators</u> B, 79/2-3, 205-213.

LIST OF CAPTIONS

1. A schematic (top-view) depiction of the stirrer. The stirrer consists of a capped conduit. The electrodes, denoted with the capital letters A, B, C, D, and E; are deposited on the conduit's bottom and they are aligned perpendicular to the conduit's walls. The electrodes are connected alternately to the positive and negative poles of a power supply. The x-coordinate is aligned along the conduit's axis. The magnetic field (denoted by dots) is normal to and points out of the page.

2. A cross-section of the conduit.

3. An estimate of the relative error resulting from truncating the infinite series after N terms. L=W=10.

4. Contours of constant stream function. The contours represent the particles' trajectories. L=W=10.

5. The horizontal component of the velocity, $u(0,y)$, is depicted as a function of y. L=W=10.

6. The vertical component of the velocity $v(x,0)$ is depicted as a function of x. L=W=10.

7. Contours of constant pressure lines. L=W=10.

8. The pressure distribution $p(x, y)$ as a function of x and y. W=L=10.

9. $v(L,0)$ is depicted as a function of L. W=L.

10. The location of the interface at various dimensionless times: t=0, 10, 20, 30, 40, and 50. W=L=10.

11. The length of the interface as a function of the normalized time.

12. The various layers of tapes that have been used for the construction of the prototype of the stirrer. Layer 1 contains the electrodes. Layer 2 contains the stirrer cavity and vertical vias for electrical connections. A few layers of type 2 were used to obtain a cavity of desired height. Layer 3 served as a cover plate. The figure is not drawn to scale.

13. A cross-section of the MHD stirrer. The layer numbers are cross-referenced with Fig. 12. Item (4) is a permanent magnet. The figure is not drawn to scale.

14. A top view of the stirrer fabricated with ceramic tapes. The cavity and the transverse electrodes are visible. At the beginning of the experiment, a thin line of dye is laid across the cavity.

15. The deformation of a dye line resulting from the application of the Lorentz forces (a). After a few seconds, the polarity of the electrodes and the direction of the Lorentz force are reversed, and the dye returns to its initial position (b). As a result of the reversal in the direction of the Lorentz force, the dye continues to deform in the opposite direction (c). When the process is allowed to continue for some time, the formation of eddies become apparent (d).
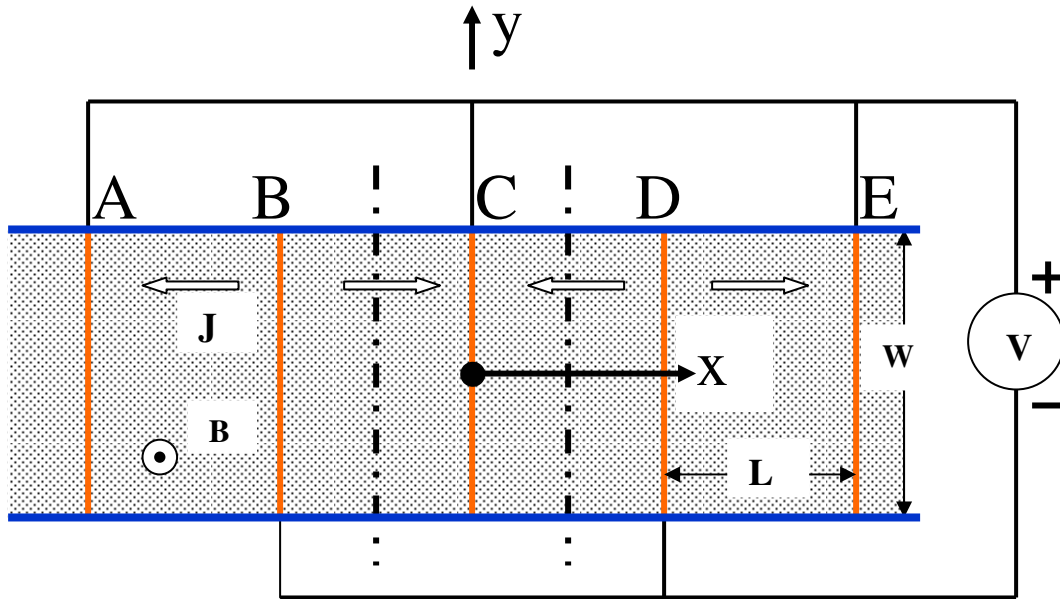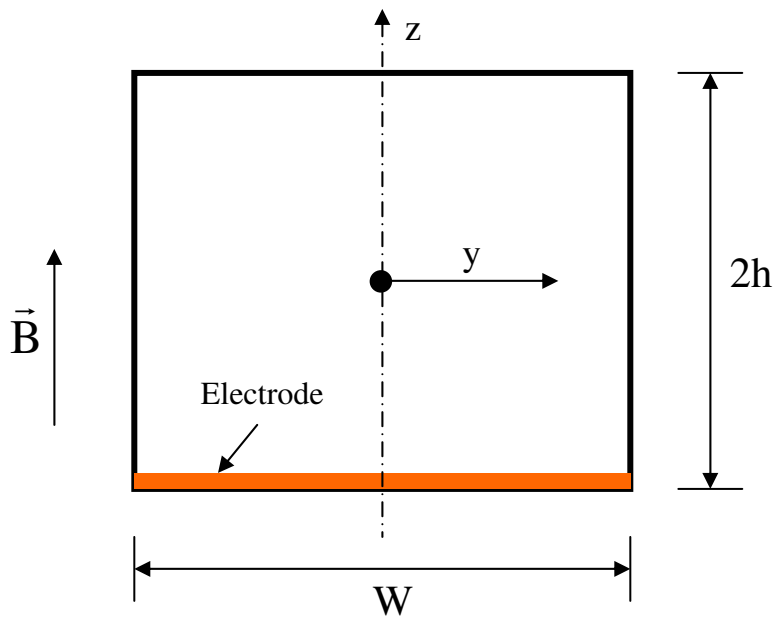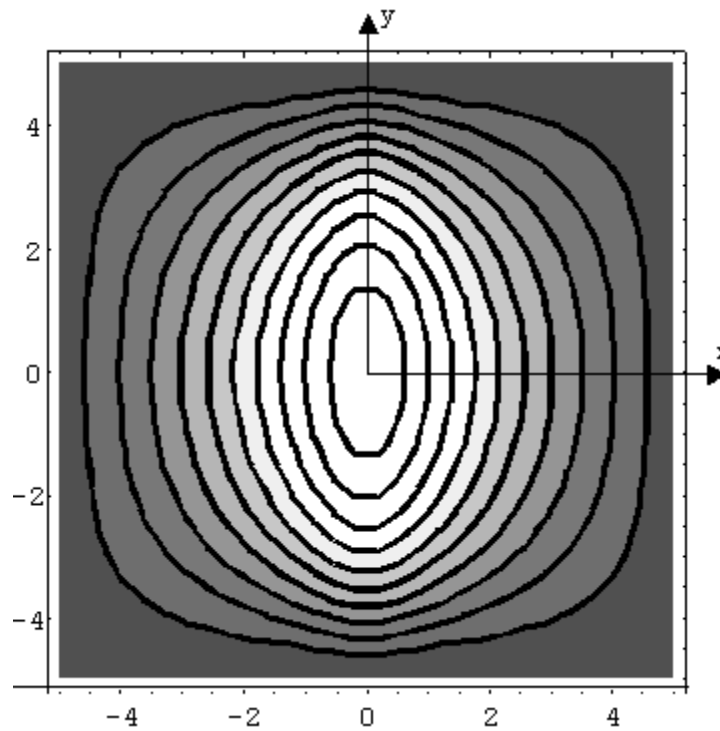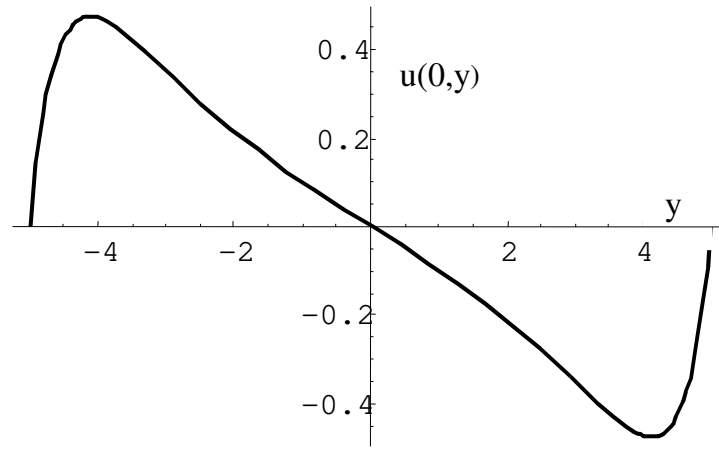
Fig. 1: A schematic (top-view) depiction of the stirrer. The stirrer consists of a capped conduit. The electrodes, denoted with the capital letters A, B, C, D, and E, are deposited on the conduit's bottom, and they are aligned perpendicular to the conduit's walls. The electrodes are connected alternately to the positive and negative poles of a power supply. The x-coordinate is aligned along the conduit's axis. The magnetic field (denoted by dots) is normal to and points out of the page.

Fig. 2: A cross-section of the conduit.
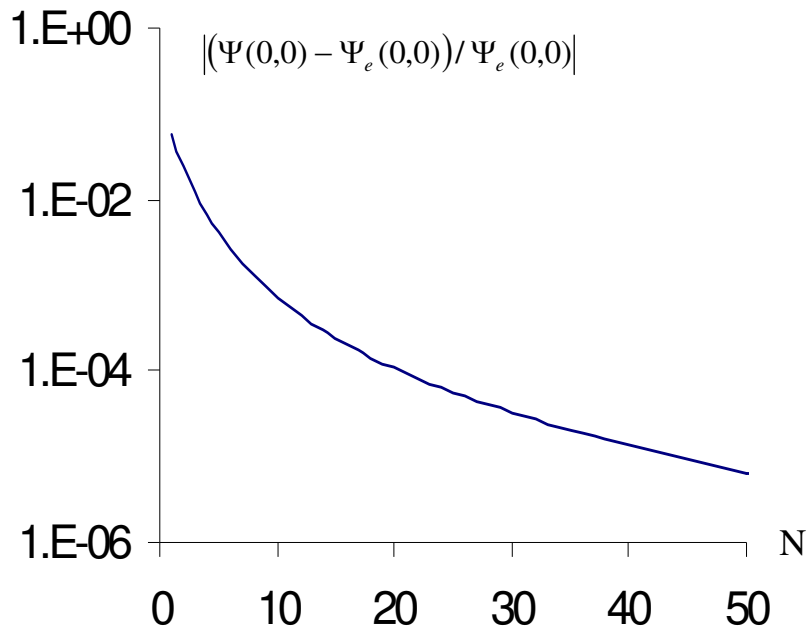
Bau, H., H., Zhong, J., and Yi, M., 2001, A Minute Magneto Hydro Dynamic (MHD) Mixer, Sensors and Actuators B, 79/2-3, 205-213.

Fig. 3: An estimate of the relative error resulting from truncating the infinite series after N terms. L=W=10.
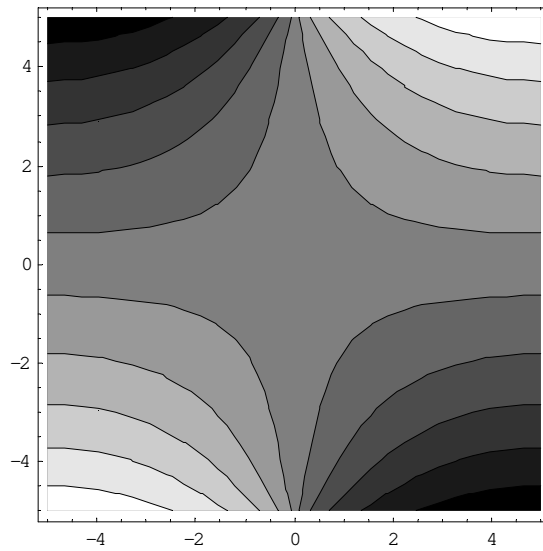

Fig. 4: Contours of constant stream function. The contours represent the particles' trajectories. L=W=10.

Bau, H., H., Zhong, J., and Yi, M., 2001, A Minute Magneto Hydro Dynamic (MHD) Mixer, Sensors and Actuators B, 79/2-3, 205-213.

Fig. 5: The horizontal component of the velocity, u(0,y), is depicted as a function of y. L=W=10.
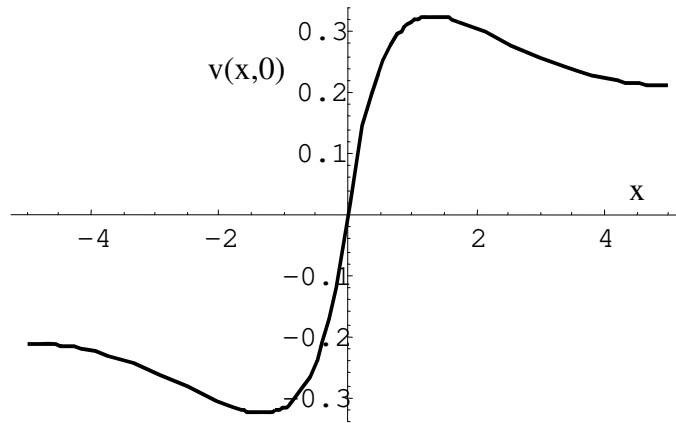
Fig. 6: The vertical component of the velocity v(x,0) is depicted as a function of x. L=W=10.

Fig. 7: Contours of constant pressure lines. L=W=10.

Bau, H., H., Zhong, J., and Yi, M., 2001, A Minute Magneto Hydro Dynamic (MHD) Mixer, <u>Sensors and Actuators</u> B, 79/2-3, 205-213.
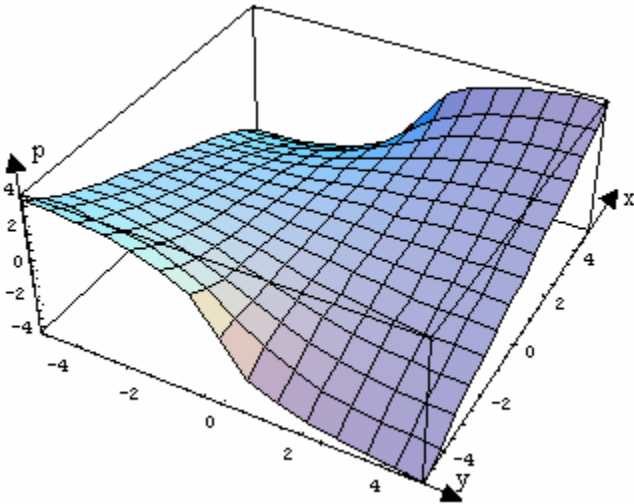
Fig. 8: The pressure distribution p(x, y) as a function of x and y. W=L=10.
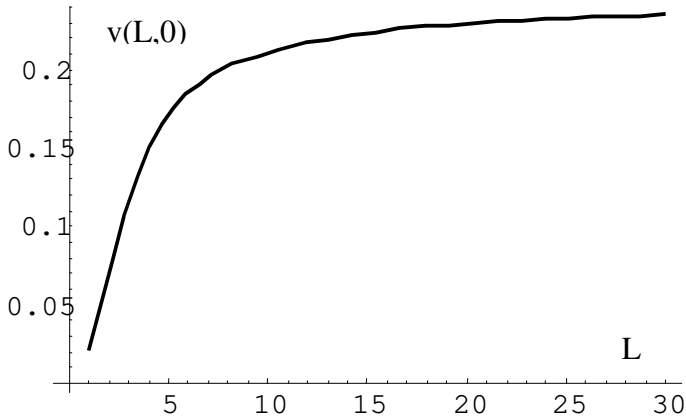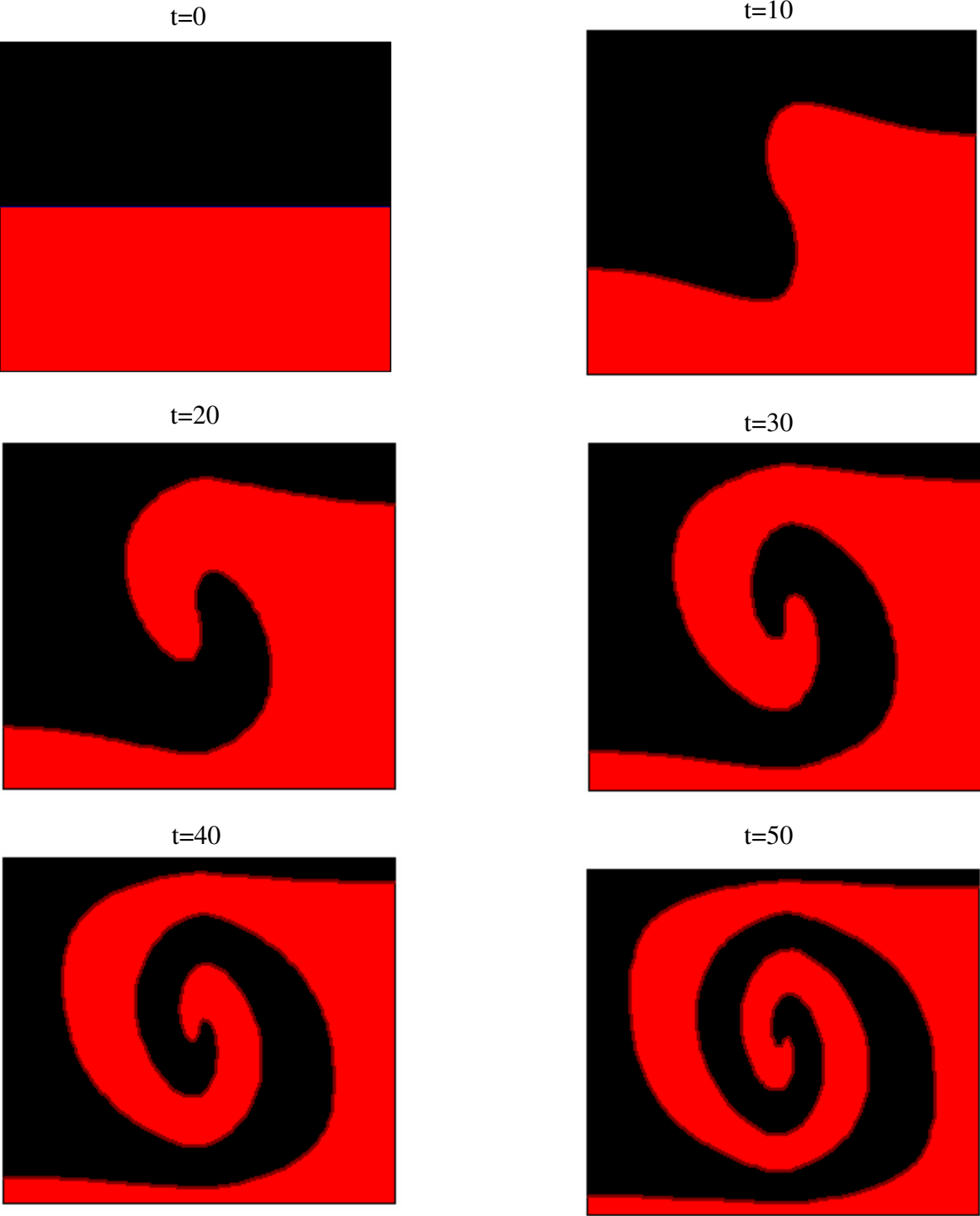

Fig. 9: v(L,0) is depicted as a function of L. W=L.

17

Bau, H., H., Zhong, J., and Yi, M., 2001, A Minute Magneto Hydro Dynamic (MHD) Mixer, Sensors and Actuators B, 79/2-3, 205-213.

Fig. 10: The location of the interface at various dimensionless times, t=0, 10, 20, 30, 40, and 50. W=L=10.

Bau, H., H., Zhong, J., and Yi, M., 2001, A Minute Magneto Hydro Dynamic (MHD) Mixer, <u>Sensors and Actuators</u> B, 79/2-3, 205-213.
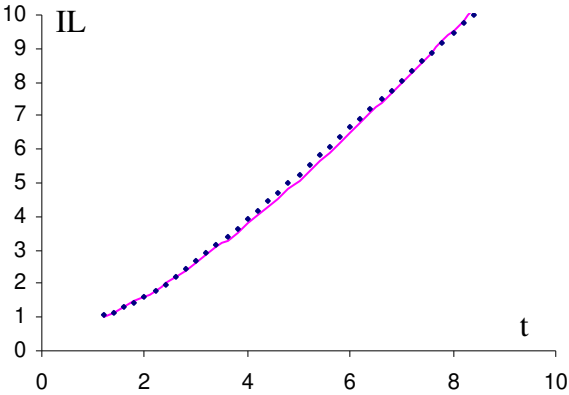
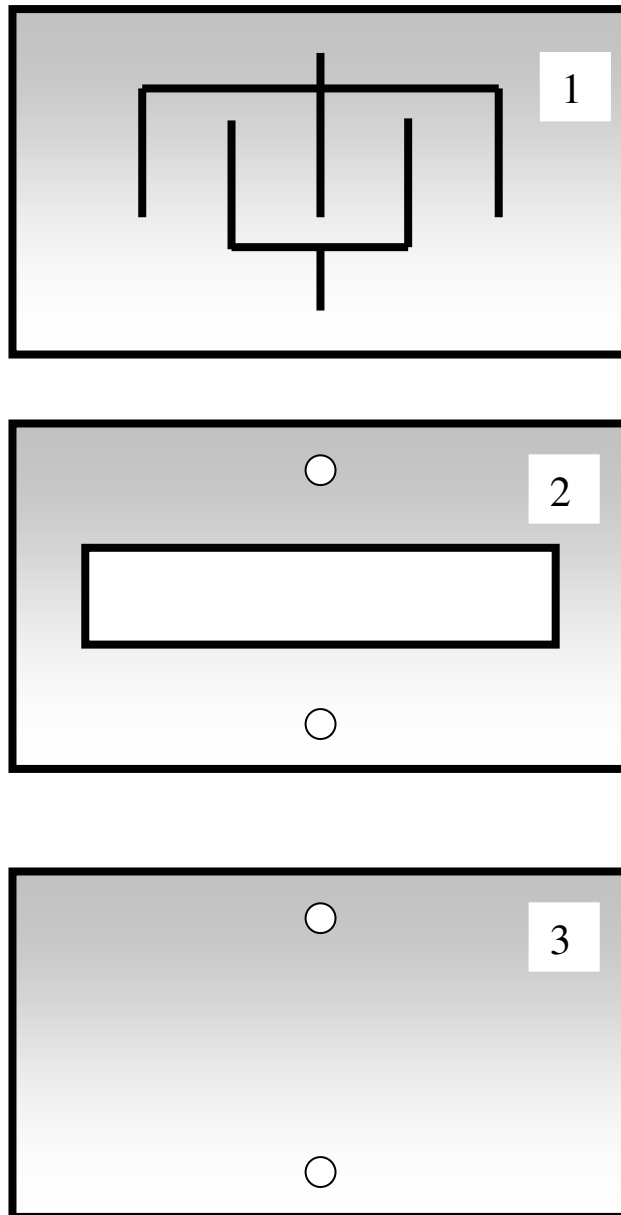Fig. 11: The length of the interface as a function of the normalized time.

Bau, H., H., Zhong, J., and Yi, M., 2001, A Minute Magneto Hydro Dynamic (MHD) Mixer, Sensors and Actuators B, 79/2-3, 205-213.

Fig. 12: The various layers of tapes that have been used for the construction of the prototype of the stirrer. Layer 1 contains the electrodes. Layer 2 contains the stirrer cavity and vertical vias for electrical connections. A few layers of type 2 were used to obtain a cavity of desired height. Layer 3 served as a cover plate. The figure is not drawn to scale.

Bau, H., H., Zhong, J., and Yi, M., 2001, A Minute Magneto Hydro Dynamic (MHD) Mixer, <u>Sensors and Actuators</u> B, 79/2-3, 205-213.
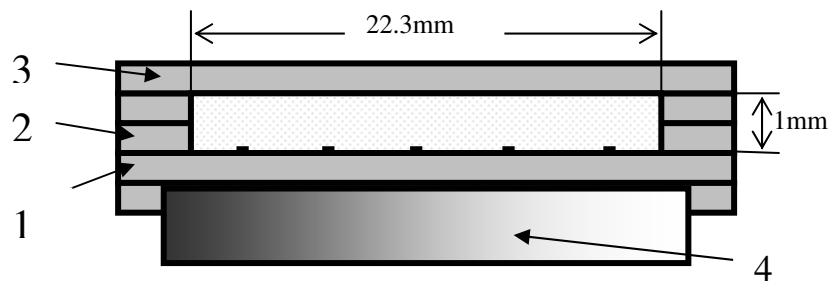

Fig. 13: A cross-section of the MHD stirrer. The layer numbers are cross-referenced with Fig. 12. Item (4) is a permanent magnet. The figure is not drawn to scale.
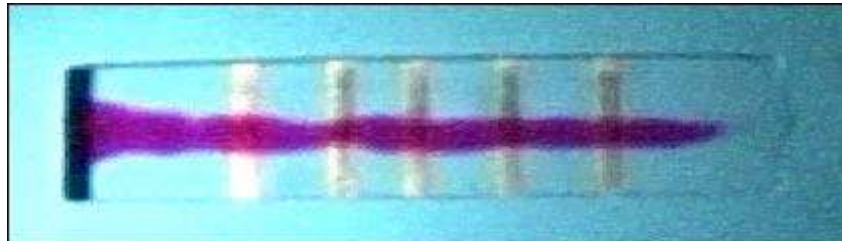

Fig. 14: A top view of the stirrer fabricated with ceramic tapes. The cavity and the transverse electrodes are visible. At the beginning of the experiment, a thin line of dye is laid across the cavity.

Bau, H., H., Zhong, J., and Yi, M., 2001, A Minute Magneto Hydro Dynamic (MHD) Mixer, Sensors and Actuators B, 79/2-3, 205-213.
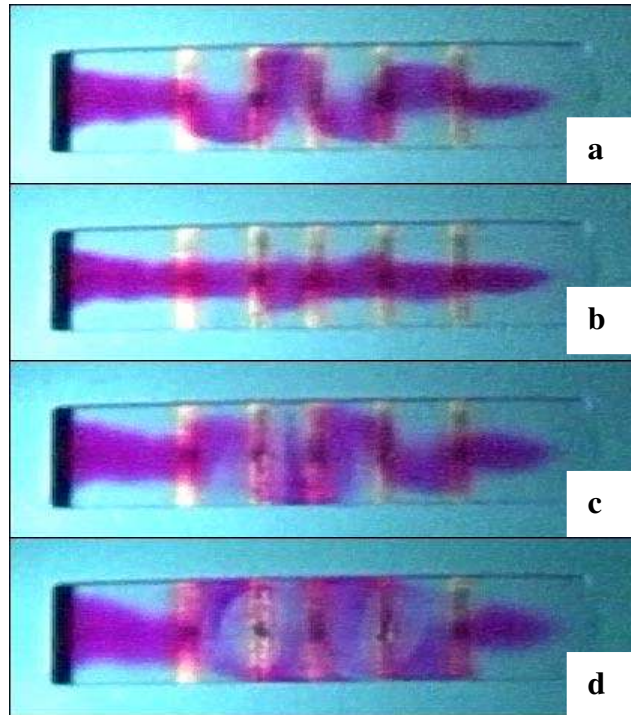
Fig. 15: The deformation of a dye line resulting from the application of the Lorentz forces (a). After a few seconds, the polarity of the electrodes and the direction of the Lorentz force are reversed, and the dye returns to its initial position (b). As a result of the reversal in the direction of the Lorentz force, the dye continues to deform in the opposite direction (c). When the process is allowed to continue for some time, the formation of eddies becomes apparent (d).